The Mari Rosa late Hercynian Sb-Au deposit, western Spain

Geology and geochemistry of the mineralizing processes

L. Ortega[1], R. Oyarzun[1,2], M. Gallego[3]

[1]Departamento de Cristalografía y Mineralogia, Facultad de C.C. Geológicas, Universidad Complutense, E-28040 Madrid, Spain
[2]Departament of Earth Sciences, The University of Leeds, Leeds LS2 9JT, UK
[3]Av. Ajalvir 8, E-28806 Madrid, Spain

Abstract. The central Iberian zone of the Hesperian Massif hosts a series of late Hercynian vein-type Sb deposits. One of them is the Mari Rosa mineralization, hosted by metagreywackes and slates of the Schist-Greywacke Complex (Upper Precambrian). The mineralization is characterized by a complex paragenesis comprising three hydrothermal stages: stage H1 → arsenopyrite-(pyrite); stage H2 → stibnite-gold; and stage H3 → pyrite-pyrrhotite-galena-sphalerite-chalcopyrite-tetrahedrite-boulangerite-stibnite. Of these only the second episode was of importance and gave rise to the main mineralized bodies of the deposit. Hydrothermal alteration consists of a mild sericitization, chloritization and carbonatization of the metasedimentary rocks around the veins. Chemical changes in the hydrothermal halos include a remarkable increase in the ratio K_2O/Na_2O, and a decrease in the ratio SiO_2/volatiles, together with a sharp increase in Sb, Mo, Au and N. Fluids associated with ore deposition lie in the H_2O-NaCl-CO_2-CH_4-N_2 compositional system. These fluids evolved, progressively cooling, from initial circulaion temperatures close to 400 °C in the early stage (H1) to temperatures of approximately 150 °C in the late one (H3). Fluid composition evolution was characterized by a progressive increase in the bulk water content of the fluids and with an increase in the relative proportion of N_2 with respect to CH_4 and CO_2 in the volatile fraction. Massive stibnite deposition resulted from a boiling process developed at 300 °C and 0.9–1 Kb at a depth of 4–5 km. Geological, geochemical and fluid inclusion evidence suggest that the intrusion of the Alburquerque batholith (late Hercynian S-type granitoids) triggered hydrothermal activity leading to the transport and deposition of Sb and Au in Mari Rosa.

The late Hercynian extensional episode (Carboniferous-Permian) was accompanied in the Iberian Peninsula by widespread plutonic activity. This magmatic activity, characterized by the intrusion of granitoids, triggered hydrothermal activity leading to one of the most outstanding metallogenic episodes of this part of Europe. Antimony veins, some of them gold bearing, represent part of the deposits formed during this episode. These antimony deposits crop out within the cores of Hercynian anticlines and are hosted by Upper Precambrian metasedimentary rocks. They all have stibnite as the main ore mineral. Genetic relationships have been suggested between some of these mineralizations and the granitoids (Gumiel 1983). However, preliminary fluid inclusion studies in the area of Mari Rosa (Fig. 1) (Ortega et al. 1991a, b) showed fluid compositions within the system H_2O-NaCl-CO_2-CH_4-N_2, thus suggesting a possible metamorphic signature (e.g. Swanenberg 1980; Kreulen and Schuiling 1982; van den Kerkhof 1988; Guillot 1989; Boiron et al. 1990). In this sense, the aim of the work was to develop a better understanding of the ore forming process from one previously selected case i.e. the Mari Rosa veins. Mari Rosa was elected as a study site because this deposit has already received some attention from a fluid inclusion studies viewpoint and moreover was considered to be representative enough of a wide number of Sb veins in western central Spain. The work required a comprehensive study, involving a reappraisal of the regional geological background, the structural control of the mineralization, the geochemistry of altered rocks, a characterization of fluid composition and evolution and an estimation of conditions for ore deposition. An integrated interpretation of these data has allowed definition of a complex metallogenical process involving fluid-rock interactions under medium PT conditions for the Sb precipitation (Ortega 1993).

Geology

The Mari Rosa deposit (Fig. 1) crops out in Upper Precambrian metasedimentary rocks affected by low-grade metamorphism. Some 8 km to the south, the Alburquerque batholith (Carboniferous) defines one of the most outstanding regional features. The intrusion of these peraluminous calc-alkaline granitoids (S-type) induced a contact metamorphism aureole some kilometers wide (Perez Cerdán et al. 1991). Early Hercynian compression defined the main deformational pattern resulting in a generalized pervasive folding and the development of a highly penetrative cleavage.

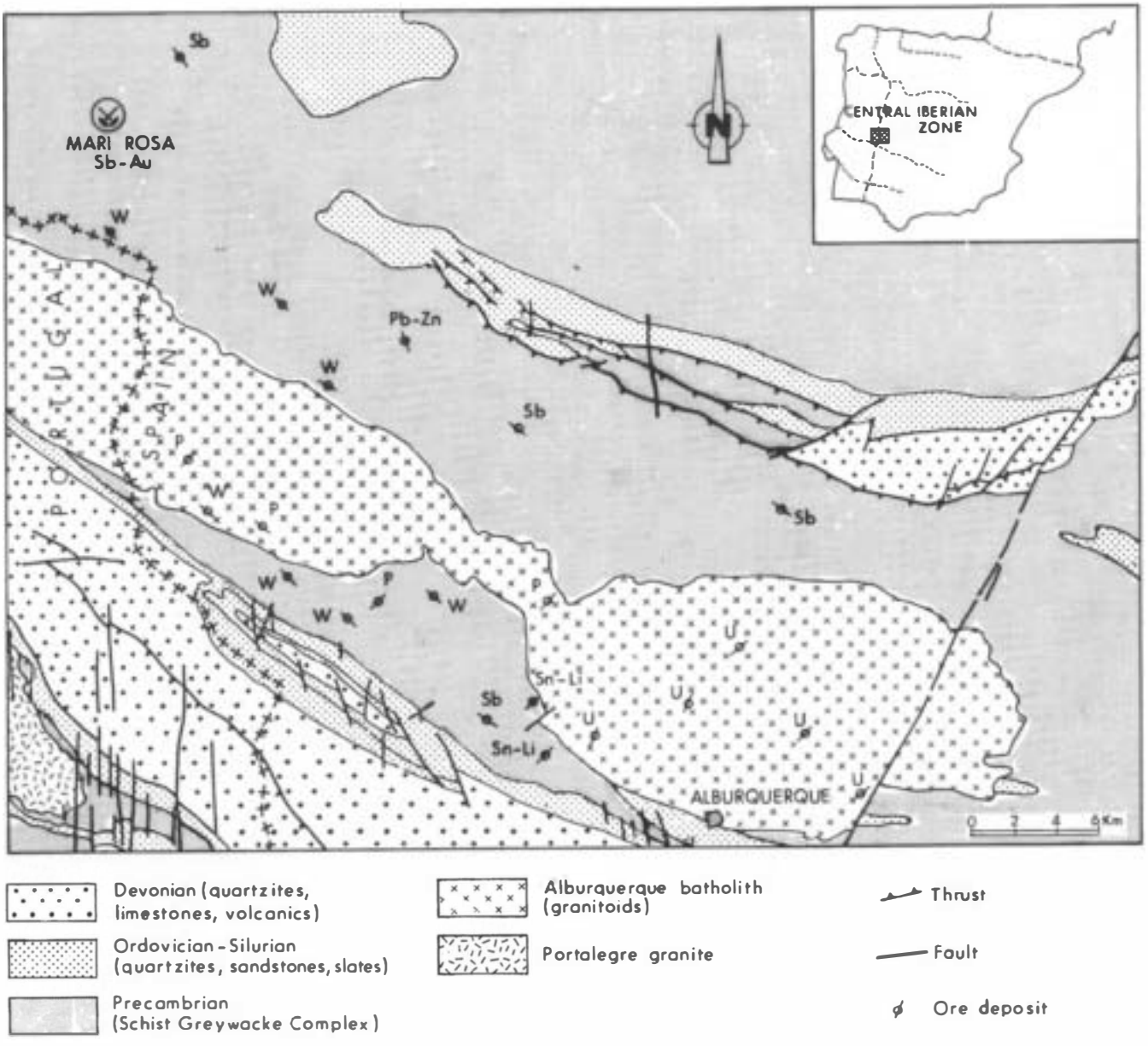

Fig. 1. Regional geologic framework of the Mari Rosa Sb-Au mineralization. Other mineralizations related to the Alburquerque Batholith are also displayed. Based on Quesada et al. (1987) and the map of the Hesperian Massif, scale 1 : 500 000 (University of Salamanca)

Host rocks

The study area is located within the central Iberian zone of the Hesperian Massif, near to its southern boundary (Fig. 1). Host rocks of the mineralization are psamitic and pelitic rocks belonging to the Schist-Greywacke Complex (Upper Precambrian). This Complex is characterized by a monotonous alternation of well-preserved metagreywackes and slates which allow for the recognition of cross-bedding, laminations and remnants of turbidite sequences (Bascones and Martín Herrero 1982). The series have been interpreted as flyschoid deposits of syn-orogenic type (Quesada et al. 1987) generated during the Cadomian compressional diastrophism. It is worth mentioning that the source of the sedimentary materials that gave rise to the Schist-Greywacke Complex might have been acid volcanic rocks of rhyolitic composition (Ortega 1993). The Complex content of immobile elements such as Y, Zr, Nb, La and Ce is strikingly similar to that one displayed by the Glass Mountain average rhyolite (Table 1; Rhyolite RGM-1, California, USA; Tatlock et al. 1976; Potts et al. 1992). This idea is also sustained by the observation of embayed quartz crystals in metagreywackes of the area of Mari Rosa which were interpreted as of possible volcanic origin (Gumiel 1983).

Three lithologies can be recognized: metagreywackes, phyllites and black slates. The metagreywackes are formed by quartz, muscovite, plagioclase and chlorite. Main accesory minerals are tourmaline, rutile, ilmenite, pyrite, apatite, zircon and monacite. The greywackes grade transitionally into phyllitic types. The phyllites are fine grained rocks characterized by a highly penetrative schistosity (S_2). The mineralogy is similar to that of the greywackes although fine muscovite (and chlorite) account for most of the matrix. The black slates are very fine grained rocks including lutitic carbonaceous bands alternating with quartz-rich layers which probably represents an original compositional banding reflecting the S_0 fabric. The S_2 fabric is well defined while S_1 can be only observed microscopically and only as a relic of an older event (Cadomian compressions).

Table 1. Average composition of the Schist Greywacke Complex (SGC) rocks in the Mari Rosa area and other volcanic and sedimentary series

	SGC	RGM-1	LP	P40136	P39803	Slates
(Weight %)						
SiO_2	72.34	73.87	69.20	71.08	75.65	–
TiO_2	0.73	0.27	0.70	0.71	0.77	–
Al_2O_3	14.37	13.80	15.00	14.59	12.08	–
Fe_2O_3	5.24	1.87	5.28	5.17	4.65	–
MnO	0.03	0.04	–	–	–	–
MgO	1.75	0.28	1.90	2.57	2.20	–
CaO	0.17	1.16	2.20	0.86	0.32	–
Na_2O	2.23	4.09	2.40	1.34	2.05	–
K_2O	2.60	4.32	3.50	3.99	2.57	–
P_2O_5	0.14	0.05	–	0.15	0.1	–
(ppm)						
Y	28	25	–	–	–	26
Zr	247	219	–	112	–	160
Nb	13	8.9	–	–	–	11
Ga	18	15	–	–	–	19
La	26	24	–	33.5	35.8	92
Ce	51	47	–	80.7	69.1	59
Cu	33	11.6	–	–	–	45
Pb	13	24	–	–	–	20
Zn	85	32	–	–	–	95
Ni	30	4.4	–	–	–	68
Mo	< 2	2.3	–	–	–	2.6
As	< 7	3	–	–	–	13
Sb	< 3	1.26	–	–	–	1.5
Au (ppb)	12	0.26	–	–	–	$\times 10^1$

RGM-1, Holocene rhyolite, Glass Mountain (USA) (Tatlock et al. 1976; Potts et al. 1992); LP, late Proterozoic clastic series; P401361, late Proterozoic-Cambrian greywackes, Antarctica; P39803, Ordovician greywackes, New Zealand (LP, P40136 and P39803 in Taylor and McLehnan 1985); Slates, after Turekian and Wedepohl (1961)

Structure

The dominant regional structural pattern in the area is Hercynian and was mainly defined by the first compressional episode. This Hercynian deformation led to similar folds with subvertical axial planes with associated penetrative cleavage (S_2). However, two other deformation episodes are also recognized in the rocks (S_1, S_3). The first cleavage is pre-Hercynian (Cadomian) and has a relic character. It can only be observed at the microscopic scale and is defined by folded quartz veinlets of variable orientation. Although this pre-Hercynian episode has already been defined (Quesada et al. 1987; Abalos and Eguiluz 1992), this is the first time that clear evidence has been presented for this deformation in an area north of the boundary separating the Ossa Morena and the central Iberian zones of the Hesperian Massif. The second cleavage (Hercynian) is highly penetrative and has a general N120°–130° trend subvertically dipping to the SW. This Hercynian episode of deformation was also accompanied by quartz veining, here defined as V_p i.e. veins parallel to the main schistosity (Fig. 2A). These veins display typical pinch-and-swell structures and were formed by quartz segregation during metamorphism. Although these veins and S_2 are clearly contemporaneous, the V_p veins have a longer structural history as revealed by mineralogical and structural studies (Ortega 1993) which demonstrated reopening and fluid circulation after the main Hercynian episodes. The third schistosity (S_3) is a crenulation cleavage affecting S_2 and corresponds to the second Hercynian episode. Minor kink-bands trending N–S and ESE–WNW are also recognized in the study area.

The late Hercynian deformation induced local compressional faults oriented N–S to N20° dipping 10°–30°E. These faults host the main stibnite bodies of Mari Rosa and are here defined as V_o i.e. veins oblique to S_2 (Fig. 2B). The faults have associated synthetic fractures, Riedel fractures (R_1 and R_2), asymetric minor folds, sigmoidal structures and gouge fabrics which indicate thrust movement along the main planes (Fig. 3). A much later fracturing produced regional strike-slip faults trending WNW–ESE, NE–SW and NW–SE.

Metamorphism

Two metamorphic episodes are recognized in the region: a pre-Hercynian one of Cadomian age and the main metamorphic episode, of Hercynian age. The first is barely recognizable and is defined by the presence of chlorite and quartz veinlets. The Hercynian metamorphism is low-grade (greenschist facies) and is characterized by the quartz-muscovite-albite-chlorite association, thus defining the chlorite zone of the greenschist facies. However, incipient development of biotite in some studied samples might reflect the transition to the biotite zone. Other temperature estimates are provided by organic matter which did not achieve graphitization, thus indicating that the regional gradient was below 350 °C–400 °C.

Even if the study area was not directly affected by the contact metamorphism induced by the intrusion of the Alburquerque batholith, a brief description of this process is worth giving here because as it will be shown later in this work, the thermal phenomena might have played a role in the local metallogenic processes. The intrusion resulted in hornblende (cordierite-andalusite-muscovite-biotite) and albite-epidote (muscovite-biotite-albite-quartz) hornfels facies around the granitoids.

The batholith

One of the major regional units in the study area is the Alburquerque batholith, a ENE–WSW lens-shaped highly differentiated

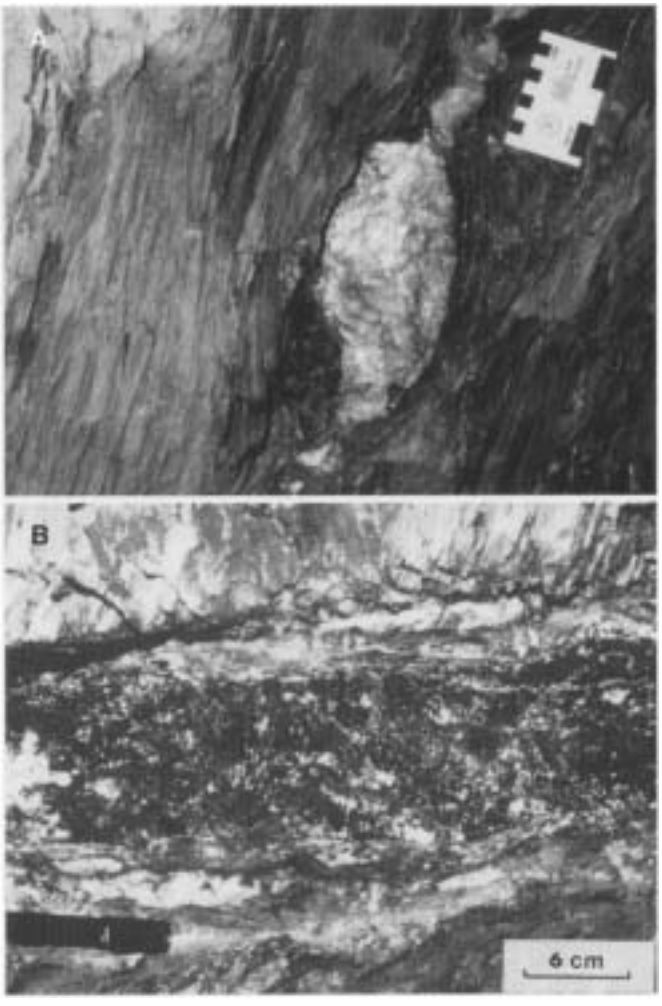

Fig. 2A, B. V_p and V_o veins, Mari Rosa mine, main drive. **A** V_p vein parallel to the S_2 main shistosity planes (S_2). Note their characteristic pinch-and-swell structures **B** V_o vein oblique to the main schistosity planes (S_2). Note the massive character of the stibnite ore

granitic mass extending for about 100 km (Fig. 1). The batholith is a complex intrusion in which two main facies can be recognized (La Roche and Marchal 1978; Santos and Casas 1982; Gallego 1992; Gallego and Gumiel 1993) : (1) two-mica porphyry granites with megacrystals of K-feldspar grading transitionally into medium to fine grained two-mica granites. This is the most important facies in terms of outcrop volume; and (2) muscovite leucogranites with minor biotite. Locally, the batholith shows a gradual outwards transition to pegmatitic dykes indicated by: (a) a change in the mica phase from biotite to muscovite and finally lepidolite; (b) a progressive substitution of K-feldspar by albite as the dominant feldspar phase; (c) a change in the type of accessory peraluminous minerals (from andalucite-cordierite to topaz-amblygonite; and (d) the existence of rare element phases together with a progressive development of pegmatitic fabrics in the external facies (Gallego 1992; Gallego and Gumiel 1993). The batholith as a whole can be defined as peraluminous calc-alkaline (S-type) with high contents of Na_2O, K_2O and P_2O_5, and low CaO (Arribas et al. 1987; Gallego 1992; Gallego and Gumiel 1993). Its age is late Westphalian/Stephanian (Rb/Sr: 286 $\pm$ 3.6 Ma, Roberts et al. 1991; K/Ar: 287 $\pm$ 10 Ma in muscovite and 293 $\pm$ 10 Ma in biotite, Penha and Arribas 1974). The batholith post-dates the Hercynian compressions but is affected by later fracturing. The granitoids can be ascribed to the late-, post-orogenic type emplaced under extensional conditions (Serrano Pinto et al. 1987; López Plaza and Martínez Catalán 1987).

The Sb-Au mineralization of Mari Rosa

Mari Rosa once represented the classic small mining operations that characterize the central Spanish landscape. Underground mining works include two drives (160 and 35 m respectively), opencast works consisted of trenching along the main structural trends. Not only antimony but gold was extracted from Mari Rosa, mainly from a gently inclined stope developed from the main drive (Gumiel 1983). Average grades of the concentrates were in the order of 62% Sb, 106 g/t Au and 34.5 g/t Ag (Gumiel 1983). Mining activities ceased in 1982. About 1.5 km to the west of Mari Rosa other mining works in the Portoviejo area reveal the existence of Sb mineralization. These consist of a 25 m deep shaft and a small mineral dump. The mineralization is found in two types of veins, already defined as V_p and V_o (Fig. 2). V_p veins are subvertical, N110°–130° trending pinch-and-swell veins (Fig. 2A) formed during the main Hercynian metamorphic-deformation event. They have a complex history of quartz segregation and later hydrothermal recrystallization accompanied by sulphide deposition. Mineralogical and structural studies allow the definition of two vein filling episodes: (1) one of Hercynian age involving quartz (Q_M) segregation along the S_2 foliation planes, and (2) a later episode of late Hercynian age which resulted in quartz (Q_H) recrystallization by hydrothermal fluids and deposition of a complex mineral paragenesis. V_o veins are hosted by N–S reverse faults which dip gently to the east. These veins are clearly late as they cross-cut the S_2 foliation and V_p veins. They carry massive stibnite-gold mineralization defining lens-shaped bodies which originated from dilational jogs along the reverse fault planes.

Mineralogy and bulk chemistry of the veins

One metamorphic and three hydrothermal stages of mineral deposition are recorded in Mari Rosa (Fig. 4). The first one is clearly Hercynian in age and resulted in barren quartz deposition (stage M: quartz, Q_M). The hydrothermal episodes are later in time and resulted in a complex paragenesis developed along three depositional stages: stage H1 → quartz (Q_{H1})-arsenopyrite-(pyrite); stage H2 → quartz (Q_{H2})-stibnite-gold; and stage H3 → quartz (Q_{H3})-pyrite-pyrrhotite-galena-sphalerite-chalcopyrite-tetrahedrite-boulangerite-stibnite. Stage H2 was the only one of economic importance giving rise to the main mineralized bodies of Mari Rosa. Quartz displays a high textural variability in the three hydrothermal stages. V_p veins contain early stretched metamorphic quartz (Q_M) almost totally recrystallized into hydrothermal quartz (Q_H) (Fig. 5). Q_{H1} is clear and occurs as relic cores surrounded by coarse-grained quartz (Q_{H2}) (Fig. 6A) in V_p veins. Dilational phenomena in V_o veins allowed formation of well-developed Q_{H2} euhedral quartz crystals intergrowth with massive stibnite (Fig. 6B). Q_{H3} is a finely crystalline quartz occurring in both V_p and V_o veins along Q_{H2} crystal boundaries and small cracks (Fig. 6A–C). These quartz generations are also well characterized from the view point of fluid evolution as they contain distinctive fluid inclusion types (see section: mineralizing fluids). Ore

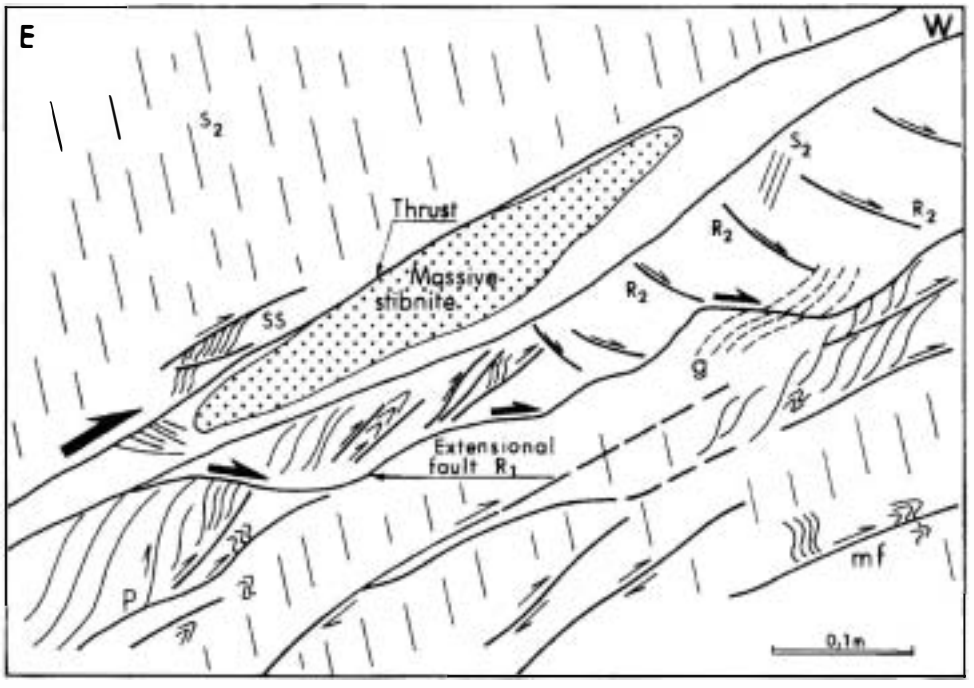

Fig. 3. Structural sketch of a V_o vein (E–W section). Four types of structures can be observed: (A) principal thrust fault, along with minor parallel planes and synthetic fractures (*P*) to the main movement surface. (B) Principal (R_1) and conjugate (R_2) Riedel fractures. (C) Assymetric minor folds (*mf*). (D) Sigmoidal structures (*ss*) and gouge fabric (*g*)

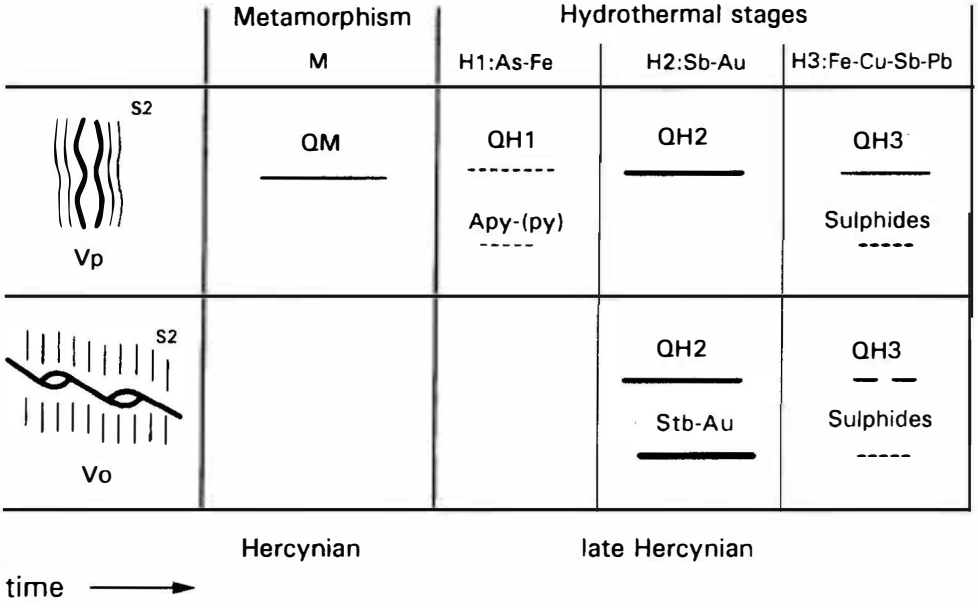

Fig. 4. Chronological relationships between the metamorphic and hydrothermal stages. S_2 main cleavage; *Apy* arsenopyrite, *py* pyrite, *Stb* stibnite, *Q* quartz

deposition resulted in a variety of textural features. Stage H1 was characterized by minor deposition of arsenopyrite in either isolated euhedral crystals (Fig. 6A) or aggregates (Fig. 7). Stage H2 gave rise to stibnite and gold. Stibnite precipitated as massive ore in V_o veins where it occurs as: (a) aggregates of anhedral twinned crystals, (2) long tabular crystals (up to 4 cm long), and (3) radiating aggregates. Euhedral quartz crystals (Q_{H2}) formed during this stage contain small isolated stibnite crystals along growth faces. In V_p veins stibnite occurs as aggregates along grain boundaries and cracks in arsenopyrite (Fig. 7). Gold occurs either within stibnite as irregular blebs or in direct contact with arsenopyrite along cracks (Fig. 7). The third stage (H3) was characterized by deposition of scattered sulphide and sulphosalt grains usually surrounded by siderite and microcrystalline quartz (Q_{H3}) (Fig. 6C).

Sb, *Mo*, *As*, *Au*, *Cu*, *Pb*, *Zn* and *Ni* account for most of the elements present in the mineralized veins (Table 2). The Sb content in V_o veins is extremely high with values of up to 35% due to the massive character of the mineralization (stage H2). In contrast, values of Sb in V_p veins are much lower because of the relative unimportance of stage H3, which resulted in minor sulphide deposition. The same applies to M_0 with values of up to 2000 ppm in the massive stibnite veins (V_o). No identification of molybdenite was made during the mineralogical studies which leads to the assumption that this mineral must be present as submicroscopic inclusions. *Au* has an extremely erratic

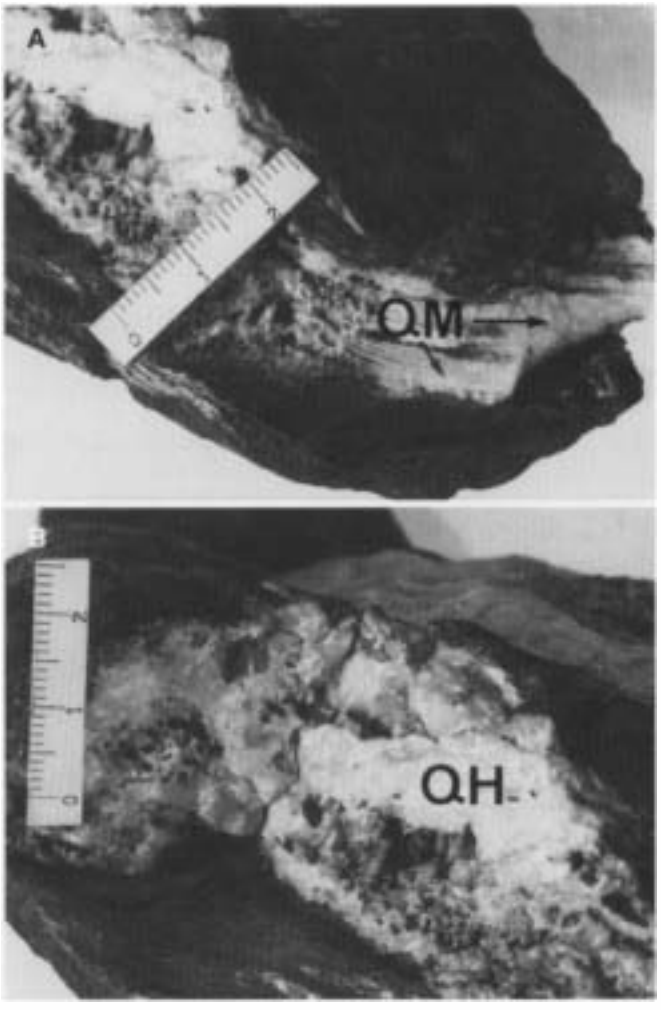

Fig. 5A, B. Hand specimen of a V_p vein showing different episodes of quartz deposition; **A** *QM*, metamorphic fibrous quartz elongated parallel to the vein direction. This fabric indicates that vein underwent stretching after metamorphic segregation yielding pinch-and-swell structures; **B** *QH*, hydrothermal quartz showing either massive or vuggy textures, typical of open space filling

distribution with most values below 20 ppb. Gold mainly concentrates in V_o veins, reaching economic values (up to 32 ppm). *As* values clearly reflect arsenopyrite deposition during stage H1. Its presence is generally low with only one analysis reaching the value of 641 ppm. *Cu*, *Pb*, *Zn*, and *Ni* have very low values in both V_p and V_o veins (< 400 ppm) also reflecting the minor importance of sulphide deposition during stage H3. High correlation values were found for the Sb-Mo and Cu-Mo pairs ($r = 0.95$ and $r = 0.96$ respectively). Gold shows a relatively high correlation with Sb ($r = 0.79$) and Mo ($r = 0.77$), while a very low value was found for the Au-As pair ($r = 0.15$) reafirming that gold was mostly deposited during stage H2, i.e., after deposition of arsenopyrite (stage H1) (Ortega 1993).

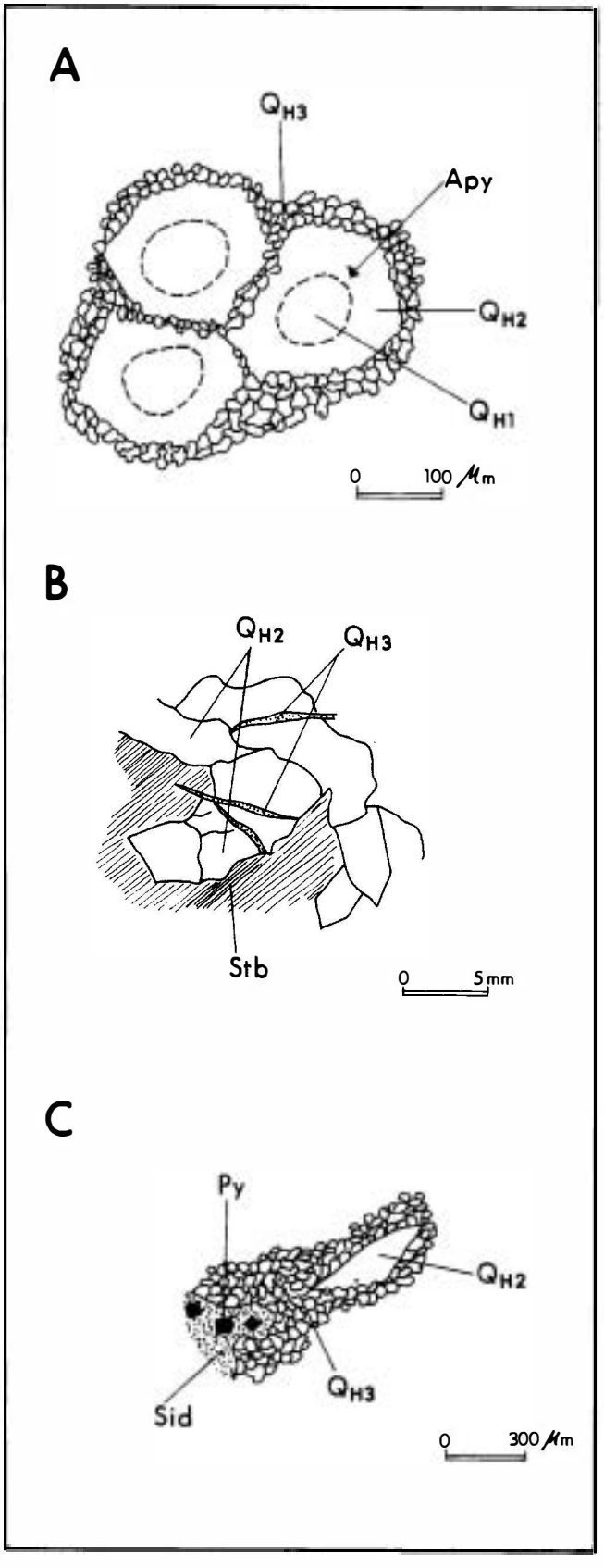

Fig. 6A–C. Sketches showing different textural relationships observed in the V_p and V_o veins mineral assemblages. **A** Cores of Q_{H1} quartz within polygonal Q_{H2} quartz containing relic isolated arsenopyrite crystals (*Apy*, stage H1) in V_p veins. Late microcrystalline quartz (Q_{H3}) occurs surrounding earlier quartz crystals. **B** intergrowth of euhedral and subhedral Q_{H2} quartz with stibnite (*Stb*, stage H2) and late Q_{H3} quartz in V_o veins. **C** microcrystalline quartz (Q_{H3}) associated with pyrite and siderite (*Py* and *Sid*, respectively, stage H3) and surrounding earlier Q_{H2} quartz

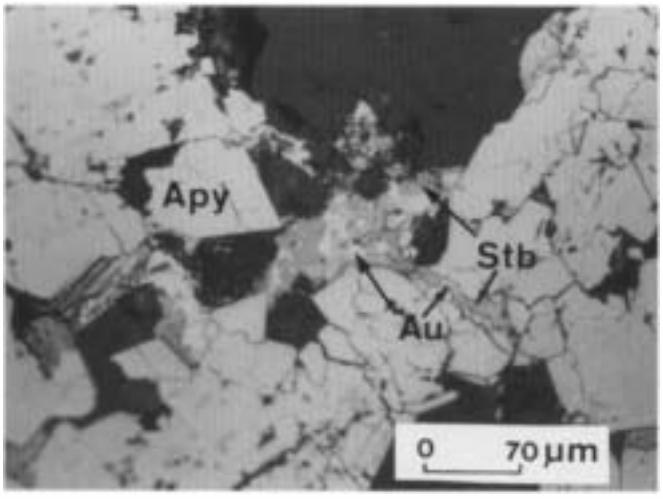

Fig. 7. Stibnite and native gold (stage H2) infilling cavities and cracks in arsenopyrite (stage H1). Reflected light under parallel polars. *Stb* Stibnite, *Au* gold, *Apy* arsenopyrite

Hydrothermal alteration

Hydrothermal alteration was neither extensive nor intensive, consisting of a mild chloritization, carbonatization and sericitization of the metasedimentary rocks around the veins. Since the metamorphic mineralogy of these rocks (fine grained muscovite, chlorite) is similar to the alteration assemblage, a multielement geochemical study was needed to characterize the actual intensity and extension of the hydrothermal phenomena. Both mineralogical and geochemical data indicate that alteration is restricted to a few centimeters around the veins.

Mineralogy

Carbonatization is the most important alteration type observed at Mari Rosa where it occurs exclusively around V_p veins and is restricted to the black slates. The carbonates vary in composition from Fe-rich to Mg-rich terms. A typical association consists in either small microlens-shaped aggregates parallel to S_2 or nodules hosting a core formed by sulphides belonging to stage H3 (pyrrhotite, galena, boulangerite, etc). Thus, the episode of carbonatization can be ascribed to the later hydrothermal stage. This type of alteration is typical of auriferous mineralizations (Boyle 1979) and has been observed in many Sb-Au deposits hosted by metapelitic rocks such as the cases of Argosy Gold Mines (Ontario, Canada), Lena Goldfields (Russia), Reefton Gold Lodes (New Zealand), Clontibret (Ireland) (Boyle 1979; Steed and Morris 1986; among others).

As stated earlier, hydrothermal chlorite and sericite were difficult to detect due to the metamorphic mineralogy of the rocks, which allowed for the clear recognition of the hydrothermal facies in only a few cases. Consequently, other tools such as the geochemical study (trace and major elements) of both the metamorphic "*unaltered*" country rocks and those surrounding the veins were used. The main results follow.

Chemistry of the alteration processes

Compared to other clastic sedimentary sequences of Upper Precambrian and Paleozoic age the rocks of the Schist-Greywacke Complex (SGC from now onwards) only differ markedly in their low CaO content (Table 1). This depletion in calcium has been observed in other metasedimentary sequences and might be a consequence of metamorphic phenomena (Shaw 1956; González-Bonorino 1971; Miyashiro 1978; Oyarzun 1982). With regards to the trace elements that actually occur in the Mari Rosa mineralization (Sb, Au, Cu, Pb, Zn, Ni, Mo, As) the contents displayed by the SGC are generally the same or slightly lower (Table 1). Thus, the rocks of the SGC unaffected by hydrothermal processes can be regarded as very representative of Upper Precambrian metasedimentary sequences and do not show significant enrichment or depletion in those metals concentrated in the mineralization.

Chemical effects of hydrothermal alteration can be expressed in terms of gains and losses in both major and trace elements (as compared to the unaltered SGC rocks,

Table 2. Trace elements in the V_p and V_o veins in Mari Rosa. Values in ppm except when % is indicated

(ppm)	Sb	Mo	As	Au	Cu	Pb	Zn	Ni	Cr	V
V_p veins										
MRG3	138	2	< 7	0.005	18	49	< 1	5	4	8
MRG16	508	6	< 7	0.018	23	373	14	3	8	9
MRG19	48	2	< 7	0.018	19	31	24	7	12	20
MRG34	< 3	2	< 7	0.004	14	4	< 1	<2	<4	<5
MRG47	4645	41	641	0.350	20	5	16	4	12	20
MRG48	116	3	39	0.013	14	<3	< 1	<2	<4	<5
V_o veins										
MRG5	> 7%	952	8	2.83	76	26	183	139	22	46
MRG13	> 12%	2215	< 7	0.023	134	126	178	189	5	28
MRG23	> 35%	2726	< 7	32.71	116	<3	35	14	5	7

<, Values under detection limit by XRF

Table 3. Average composition of different rock groups in the Mari Rosa area

	SGC	MRG40	Host rocks	V_pC	V_oC	V_oC^*
(Weight %)						
SiO_2	70.42	62.65	67.82	56.67	61.15	65.06
TiO_2	0.71	0.85	0.73	1.00	0.57	0.60
Al_2O_3	13.97	17.50	15.76	21.85	14.52	15.38
Fe_2O_3T	5.10	6.66	4.95	6.33	4.56	4.92
MnO	0.03	0.03	0.03	0.02	0.01	0.01
MgO	1.70	2.52	1.39	1.86	0.64	0.68
CaO	0.17	0.31	0.13	0.13	0.08	0.09
Na_2O	2.16	2.24	2.07	1.36	1.20	1.24
K_2O	2.53	3.34	3.31	5.56	3.03	3.20
P_2O_5	0.13	0.16	0.13	0.18	0.10	0.10
LOI	2.67	3.53	2.98	4.45	3.49	3.25
(ppm)						
Sb	< 3	< 3	73.6	132.3	> 16168	–
Mo	< 2	< 2	2.6	3.0	132.4	–
As	< 7	< 7	8.9	11.5	26.4	–
Au	0.009	0.01	0.007	0.008	0.23	–
Cu	32.6	42	32.9	43.2	71.0	–
Pb	13.1	14	13.1	59.0	31.0	–
Zn	82.3	109	78.3	115.3	110.5	–
Ni	28.4	44	27.2	38.8	54.6	–
Cr	74.5	101	75.7	122.3	129.0	–
V	107.5	157	116.2	182.1	135.9	–
Rb	87.4	118	109.8	182.6	100.2	–
Sr	63.6	78	63.0	60.0	47.9	–
Ba	452.3	579	545.0	909.5	533.0	–
Y	25.0	33	30.4	39.5	28.8	–
Zr	238.6	196	217.3	276.5	200.8	–
Nb	12.8	15	13.3	17.5	12.5	–
Th	8.0	9	7.9	10.2	2.7	–
La	26.1	27	25.3	35.2	3.1	–
Ce	51.1	51	52.4	76.0	46.6	–
Ga	17.9	23	20.4	28.6	20.8	–

SGC, Schist Greywacke Complex, regional samples; MRG40, black slate regional sample; Host rocks, samples from the main drive of the mine; V_pC and V_oC, V_p and V_o contact zones; V_oC^*, V_oC average (Total = 89.36%), recalculated without antimony

Table 3). These changes can be summarized as follows:

1. Depletion: CaO, MgO, Na_2O, MnO, (Al_2O_3)
2. Enrichment: K_2O, volatiles
3. No variation: SiO_2, Fe_2O_3T

Even if these trends are similar in the V_p and V_o surroundings, the intensity of the alteration is different, being generally higher near to the V_p veins. It should be noted that these zones were affected by an earlier hydrothermal stage (H1) that predates V_o formation.

These chemical changes are very similar to those described as typical of hydrothermal alteration associated with Au-Sb vein type deposits (Boyle 1982; Cruzat 1984). However, the low reactive potential of rocks such as greywackes and phyllites (Boyle 1982) results in very mild alteration effects. Thus, the hydrothermal transformation is often better defined if ratios between elements rather than individual behaviors are considered. In this sense, the ratios K_2O/Na_2O and SiO_2/volatiles can be used as clear-cut indicators of the extension and magnitude of the hydrothermal alteration in gold-antimony deposits (Boyle 1974, 1982; Cruzat 1984). In the case of Mari Rosa, the alteration is characterized by a remarkable increase of K_2O/Na_2O and a decrease of SiO_2/volatiles mostly restricted to the vicinity of the veins (Fig. 8).

Among the trace elements, only Sb, Mo and As show a progressive and continuous enrichment towards the mineralized veins (Table 3). The increase is outstanding for antimony which concentrates up to 10 000 times more than the average of the regional unaltered rocks of the SGC whilst Mo reaches up to 60 times more than the regional value. These two elements have an excellent correlaion ($r = 0.9$) in the altered rocks (Fig. 9). Gold shows an extremely erratic behavior, having however a maximum concentration close to the V_o veins (up to 0.23 ppm against a regional background of 9 ppb). Cu, Pb, Zn and Ni only show slight increases close to mineralized veins.

The mild character of the alteration is also reflected in the poor variation observed in the contents of Rb and Sr, two elements which are highly mobile during hydrothermal processes (Oyarzún 1974; Armbrust et al. 1977). Cr, V, Ba, Y, Zr, Nb, Th, La, Ce and Ga do not show any significant enrichment/depletion trend, which agrees with the generally immobile character of these elements.

Since preliminary fluid inclusion studies showed that N_2 and CH_4 were important components of the fluid phase (Ortega et al. 1991b), nitrogen and carbon were considered to be useful in characterizing the fluid-rock interactions. Elemental N concentrations in the studied samples

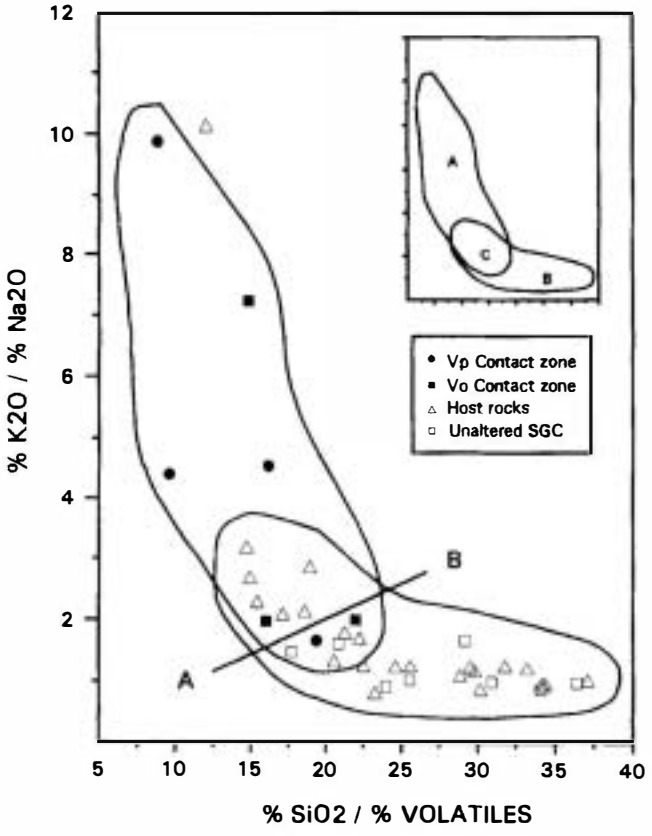

Fig. 8. K_2O/Na_2O versus SiO_2/volatiles diagram. *Zone A* Altered rocks corresponding to the vein contact zones. *Zones B* Host rocks and unaltered Schist Greywacke Complex samples. *Zone C* Includes host rocks showing hydrothermal alteration according to the chemical ratios used as markers. *AB line* Boundray separating altered and unaltered samples

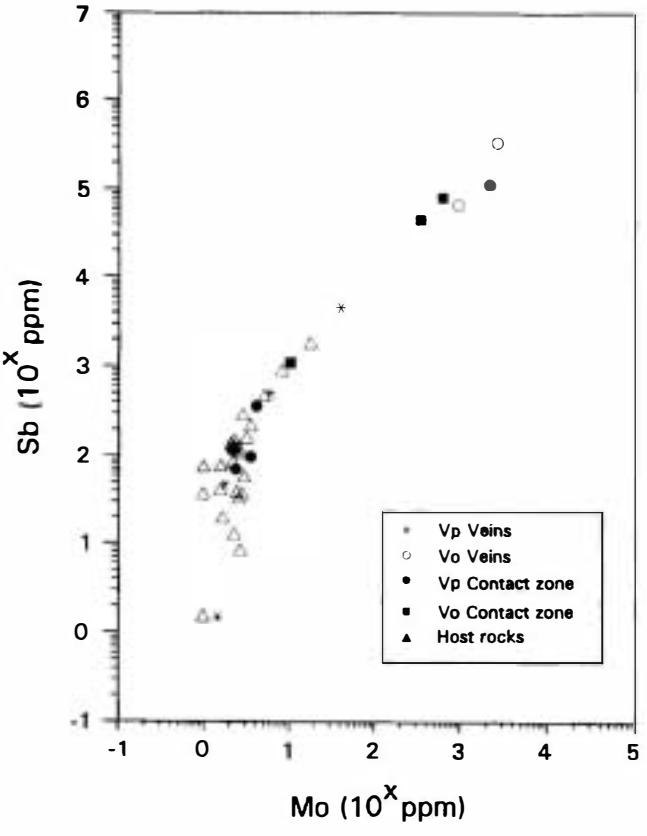

Fig. 9. Variation diagram of Sb versus Mo in V_p and V_o veins and in the host rocks

range from 200 to 2300 ppm (Fig. 10A). Unaltered samples of the SGC display a value around 800 ppm N. Organic carbon ranges from 100 to 3200 ppm (Fig. 10B). The highest values of N are observed in the altered rocks surrounding V_p and V_o veins (up to 2200 ppm N) which correlates with the K_2O/Na_2O index (Fig. 10A). Organic carbon contents are mainly controlled by lithology, recording maximum values in black shales which host V_p veins. The plot of C versus N shows a total absence of correlation between them (Fig. 10B). This together with high values observed in the altered rocks might indicate that at least part of the nitrogen did not result from the decay of organic mater but was externally derived and introduced into the system by hydrothermal fluids (Ortega 1993).

Mineralizing fluids

Four types of fluid inclusions have been observed in quartz samples from V_p and V_o veins. Their microthermometric and Raman data are summarized in Table 4 and Fig. 9. Types I, II and IV correspond to biphase water-bearing inclusions, while type III is volatile-rich and typically appear monophase at room temperature. The volatile's composition belongs to the system CO_2-CH_4-N_2, with variable proportions of each component depending upon the inclusion type. Relative chronology of the inclusions is well established (Fig. 11; Ortega et al. 1991b; Ortega 1993). Type I is the earliest inclusions and occurs in clear cores of quartz crystals in V_p veins, predating the V_o veins formation. Types II and III are primary inclusions in V_o veins and show good evidence of being trapped contemporaneously: both type II and III occur delimiting the growth faces of idiomorphic quartz, either sharing the same planar arrays or within different but parallel alignments. These two types of inclusions are coeval and secondary within V_p veins. Type IV inclusions occur in healed fractures in all the samples and are secondary.

The general trend of homogenization temperatures reveals a decrease from 390 °C in the early stage (H1) to 150 °C in the late stage (H3) (Table 5; Fig. 12). Stibnite precipitation took place in the second hydrothermal episode, with homogenization temperatures ranging from 180 °C to 330 °C. Salinity estimations for stages H2 [Note that for type II inclusions (Stage H2) complex clathrates affect microthermetric data although maxima values of salinity can be estimated from ice melting temperatures.] and H3 range between 3 and 9% eq. wt.% NaCl (Fig. 12). No data are available for stage H1 due to complex clathrate formation and lack of ice melting temperatures. Fluid composition follows a continuous trend of evolution characterized by a progressive increase in the bulk water content of the fluids and an increase in the relative proportion of N_2 with respect to CH_4 and CO_2 in the volatile fraction. This steady evolution of the system (Table 4)

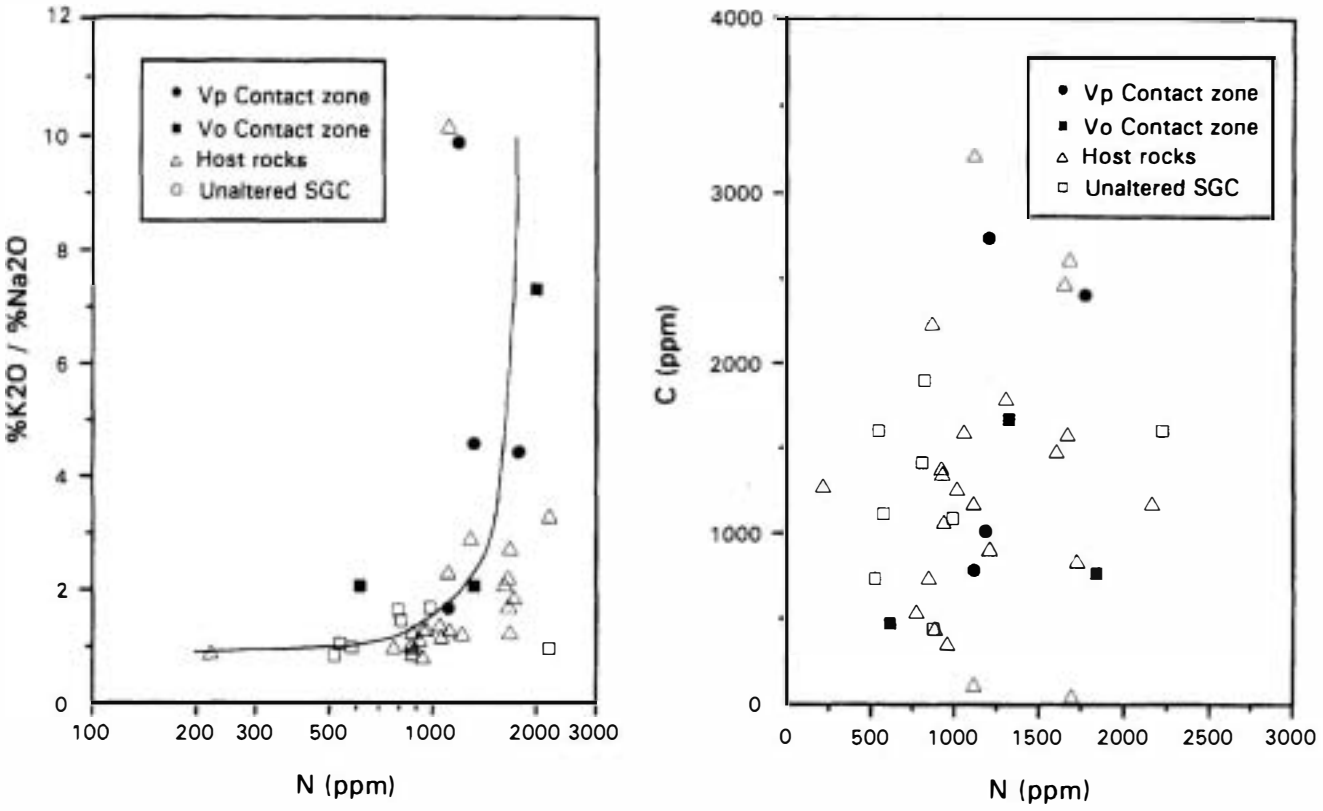

Fig. 10. Nitrogen distribution versus the alteration index K_2O/Na_2O in altered and unaltered rocks (*left panel*). Nitrogen versus organic carbon. Nitrogen and organic carbon were analyzed with a Carlo Erba EA 1108 Elemental Analyzer (University of Southampton) (*right panel*)

Table 4. Microthermometric and Raman data for fluid inclusions in quartz from V_p and V_o veins. Microthermometry performed on a Chaixmeca heating-freezing stage; Raman spectroscopic analyses were obtained with a Jobin-Yvon MOLE Raman microprobe (BRGM, Orleans; France). Salinity estimated from Tm ice

	Microthermometric data	Raman data
Type I	Vv/Vt: 0.4 to 0.6 T_mCO_2: −73.5 to −61 °C T_hCO_2: −45 to −19 °C (V) $T_m$ice: not available T_mCl: 9.5 to 14.5 °C Salinity: not available TH: 275 to 377 °C (L)	CO_2: 34 to 61% CH_4: 29 to 43% N_2: 10 to 23%
Type II	Vv/Vt: 0.15 to 0.25 $T_m$ice: −6 to −2 °C Salinity: 3 to 9% eq. NaCl T_mCl: 5 to 8 °C TH: 190 to 330 °C (L) TD*: 230 to 310 °C	CO_2: 29 to 41% CH_4: 9 to 23% N_2: 43 to 60%
Type III	Vv/Vt: > 0.9 $T_h(CH_4$-$N_2)$: −138 to −121 °C (L, V, C) T_mCO_2: −77.2 to −66 °C	CO_2: 14 to 21% CH_4: 18 to 28% N_2: 56 to 64%
Type IV	Vv/Vt: < 0.1 $T_m$ice: −5.2 to −1.5 °C Salinity: 2.5 to 9% eq. NaCl TH: 160 to 266 °C (L)	CO_2: n.d. CH_4: 23 to 24% N_2: 76 to 77%

TD, Temperature of decrepitation *before* homogenization;
TH, temperature of total homogenization;
Th, temperature of partial homogenization

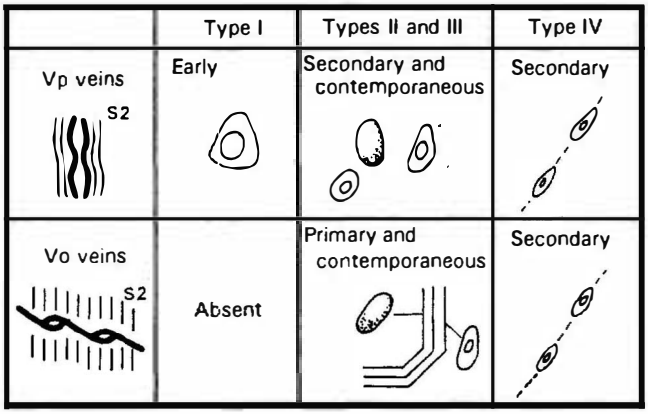

Fig. 11. Chronology and distribution of the different types of fluid inclusions in the V_p and V_o veins

suggests that only one fluid was involved. As pointed out before, the supply of nitrogen to the fluids can originate in organic matter and/or ammonium-bearing silicates in surrounding pelitic rocks (Dubessy and Ramboz 1986; Guillot 1989).

The hydrothermal process can be reconstructed as follows. The early stage (H1) is characterized by aqueous carbonic fluids ($CH_4 \pm CO_2$) circulating at minimum temperatures of 300 ± 50 °C (Table 5). This episode is mostly barren, with only minor arsenopyrite-(pyrite).

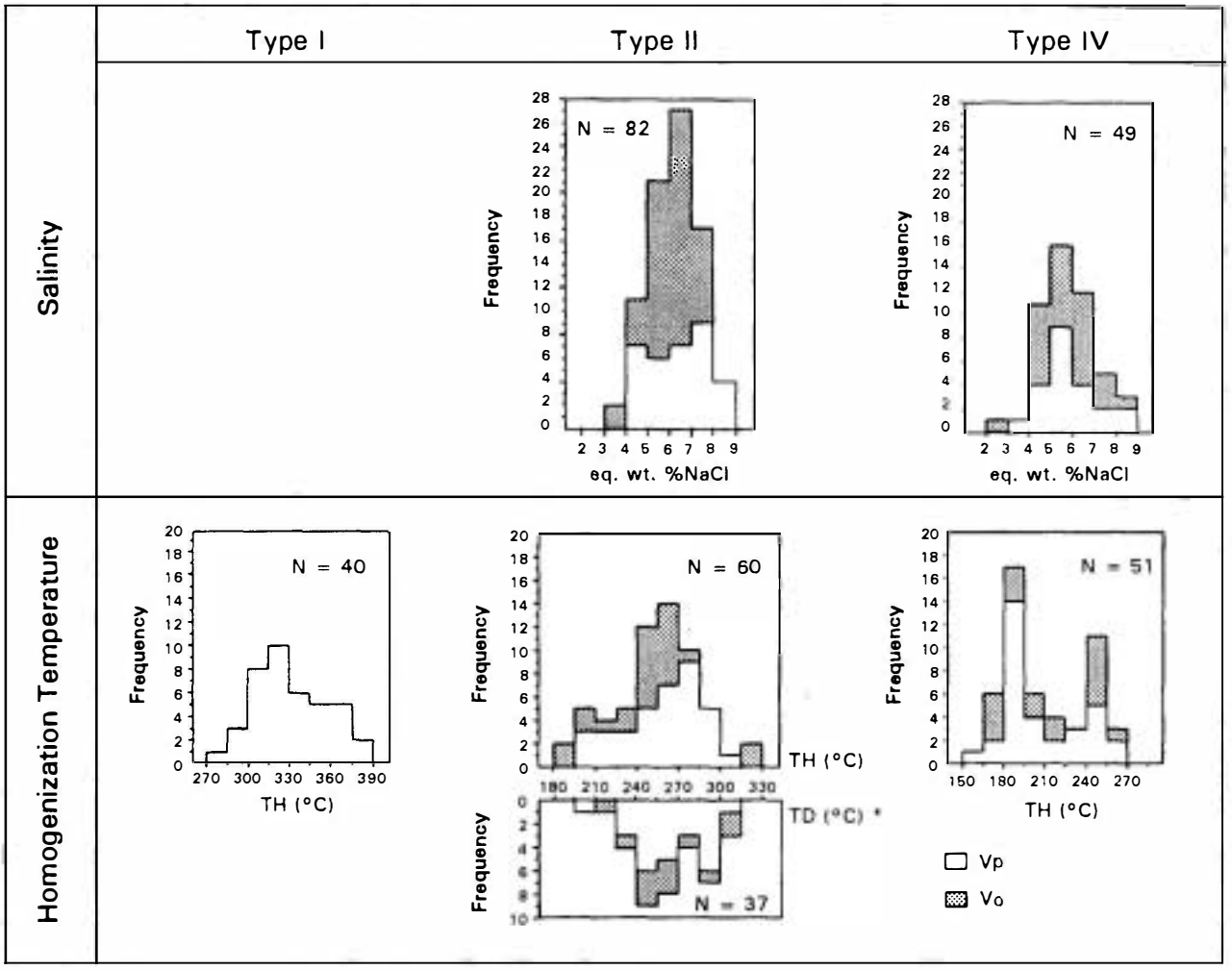

Fig. 12. Salinities (eq. wt.% NaCl) and homogenization temperatures (*TH*) in the different types of water-bearing fluid inclusions. For type II inclusions, salinity data estimated from Tm ice are maxima values. *TD* Temperatures of decrepitation *before* homogenization

Table 5. Characteristics of the mineralizing fluids associated to the different hydrothermal stages

Hydrothermal stages	Mineralizing fluids	
	T_H	Composition
H1: Q-As-Fe	270°–390 °C	H_2O-(NaCl)-CO_2-CH_4-(N_2)
H2: Q-Sb-Au	180°–330 °C	H_2O-NaCl(<9%)-CO_2-CH_4-N_2 + N_2-(CO_2-CH_4)[a]
H3: Q-Fe-Cu-Sb-Pb	150°–270 °C	H_2O-NaCl(<9%)-N_2-(CH_4)

[a]Composition of the liquid-rich and vapor-rich fluids unmixed during boiling

The second stage (H2) is the main mineralizing episode and led to the deposition of gold-bearing massive stibnite. This stage is characterized by the immiscibility of the fluid, as demonstrated by the coexistence of liquid-rich (type II) and vapor-rich (type III) inclusions, which represent the unmixed parts of the previously homogeneous fluid. In this process the more volatile components are preferently partitioned towards the vapor fraction resulting in a higher concentration of CH_4 and N_2 in the type III V-rich inclusions (Table 4). Interpretation of the fluid inclusion data in terms of immiscibility in this deposit have been discussed in Ortega et al. (1991b) and Ortega (1993) and constrain the probable *PT* conditions for the boiling event at around 0.9–1 kbar and 300 °C. Such a process was triggered by sudden pressure drops in dilational jogs (V_o veins) developed during thrust movement (Fig. 3). Dilational jogs as defined by Sibson (1987, 1990) and Sibson et al. (1988) are localized zones of extension arising from fault curvature or en echelon segmentation. They form particularly favorable depositional sites (e.g., Mari Rosa V_o veins, Fig. 2B) characterized by rapid pressure drops between rupturing episodes (Sibson 1987, 1990; Sibson et al. 1988). Close textural relationships between stibnite and idiomorphic quartz grown during boiling demonstrate that unmixing or exsolution is the driving mechanism for massive stibnite precipitation in V_o veins. Boiling fluids modelling by Spycher and Reed (1989) shows that no significant concentrations of antimony fractionate into the gas phase upon at least 97% of the solution at or

below 300 °C. These calculations have been carried out for a geothermal system, such as Broadland (New Zealand), with fluid compositions and pressures that differ from those of Mari Rosa. Therefore, these figures should be taken as an approach to the problem only. Based on this, it may be proposed that during the fluid phase separation at Mari Rosa, metals concentrated within the liquid fraction, reaching a strong supersaturation in antimony. This would induce the sudden desestabilization of antimony complexes, triggering the massive precipitation of an important volume of stibnite in a short time span. This process could have been sustained for as long as the cavities remained opened to the circulation of fluids.

As stated, massive stibnite mineralization is mainly confined to V_o veins. Both type II and type III inclusions, representative of this boiling episode, were trapped in V_p veins, however only very minor stibnite was deposited. This fact indicates that type II and III fluids were already barren differentiated phases when circulating along the V_p veins. In fact, V_p veins became mineralized only in those places where they are cross-cut by V_o. Therefore, unmixing was mainly controlled by the opening of dilational jogs (V_o veins) and subsequent pressure drops which occurred within low angle thrusts.

Finally, the third hydrothermal stage (H3) is characterized by mainly aqueous fluids. Volatiles, when detected, show a maximum enrichment in nitrogen with respect to previous stages (Table 4). Type IV inclusions are probably derived from the liquid fraction after boiling and represent the deposition of a wide variety of sulphides and sulphosalts of Cu, Fe, Sb and Pb (Table 5). They show two modes of homogenization temperatures at around 250°C and 190 °C (Fig. 12). The upper temperature limit for this late stage is defined by the previous boiling episode at 300 °C and probably it was not higher than 270 °C (maximum TH; Fig. 12). No major changes in salinity are registered from stage H2 (liquid-rich fluid) to stage H3 in this deposit.

Discussion

Several facts made the origin of the Mari Rosa antimony mineralization rather dubious until now. A complex mineral paragenesis deposited by solutions containing the ubiquitous presence of CH_4 and N_2 suggested a possible metamorphic signature for the deposit (e.g., Swanenberg 1980; Kreulen and Schuiling 1982; van den Kerkhof 1988; Guillot 1989; Boiron et al. 1990). Furthermore, part of the mineralization (V_p veins) was clearly hosted by structures developed during the main Hercynian compressional episode. Besides, recent studies in the French Central Massif (a Hercynian unit equivalent to the Hesperian Massif in many aspects) for the Salsigne deposit suggest a complex metallogenic evolution involving metamorphic and hydrothermal stages (Boiron et al. 1990). Since V_p and V_o veins were clearly distinct, at first sight, a similar hypothesis for Mari Rosa could be made i.e., a first Hercynian stage involving mineral deposition in V_p veins followed by a late Hercynian hydrothermal stage resulting in massive stibnite deposition in the newly formed V_o veins.

Thus so far, these are what could be termed the metamorphic and metamorphic-hydrothermal hypotheses for Mari Rosa. However, apart from these ideas, largely based on fluid inclusion and preliminary structural data, the influence of the Alburquerque batholith was yet to be determined. This is particularly relevant if we take into account that a series of mineralizations (some of them Sb deposits) within and surrounding the batholith are genetically related to the intrusion (Fig. 1; Gumiel and Arribas 1987; Gumiel and Gallego 1991; Gallego and Gumiel 1993). Thus, a third hypothesis for Mari Rosa can be proposed: mineral deposition in relation to a hydrothermal system driven by the late Hercynian granitic intrusion. Even if the nearest granitic outcrops are some 8 km away from Mari Rosa two major points should be taken into account: (1) until very recently (Pérez Cerdán et al. 1991) the hidden shape of the batholith was generally unknown and (2) the intrusion of the batholith in late Hercynian time must have resulted in a thermal surge increasing the geothermal gradient up to a point to trigger hydrothermal activity at a regional scale.

Mari Rosa and the Alburquerque batholith: more than pure spatial relationships?

The proximity of Mari Rosa to the Alburquerque batholith gives rise to many questions regarding the possible cause-effect relationships between them. If the granitic intrusion was actually involved in the mineralizing process, then its role can be understood in terms of: (1) a thermal source to trigger and drive the hydrothermal system; (2) a source for the fluids and (3) a source of both fluids and metals.

A first insight into the problem comes from the series of mineralizations within and around the Alburquerque batholith (U, P, Li, Sn-W, Sb and Pb-Zn; Fig. 1), clearly indicating the major metallogenic role of the intrusive rocks (Gumiel et al. 1976; Gumiel and Arribas 1987; Gumiel and Gallego 1991; Gallego and Gumiel 1993). Second, even if the distance between Mari Rosa and the batholith outcrops is relatively large, the northern boundary of the batholith does not fall vertically but rather dips gently to the north as revealed by a sharp increase in the width of the metamorphic aureole towards the NW (Pérez Cerdán et al. 1991). Thus, the deposit and the granitic rocks are actually very much closer than mere surface mapping would suggest.

Another point to be taken into account comes from the study of the nitrogen and organic carbon distribution in the altered rocks. As already mentioned these two elements do not correlate, thus implicitly indicting that mere organic matter decay cannot account for the observed N values in the altered rocks. Furthermore, nitrogen content increases in altered rocks with respect to the regional values, suggesting that hydrothermal fluids played a major role in the N enrichment close to the veins, introducing additional nitrogen from an external source. Minimal thermal conditions to liberate nitrogen (NH_4^+) from micas fall within the range 550–600 °C (Hallam and Eugster 1976). Since fluid circulation around the veins did not reach values higher than 400 °C, the NH_4^+ source must be

searched for further away, within an area where temperatures between 550–600 °C could have developed allowing a combination of metamorphic and hydrothermal phenomena. The inner contact metamorphic aureole (hornblende hornfels facies) of the Alburquerque batholith can be regarded as the most probable site for nitrogen hydrothermal leaching. Similar processes are now well described from the geochemistry and mineralogy viewpoint (Wilkinson 1991; Hall et al. 1991). Thus, a simple process involving the following steps can be proposed for the nitrogen enrichment around the V_p and V_o veins: (1) hydrothermal leaching of N from the internal zone of contact metamorphism involving both metamorphic and hydrothermal phenomena around the batholith; (2) transport of nitrogen towards the mineralization site; (3) circulation of nitrogen-bearing fluids within the vein system (as revealed by the fluid inclusion study); and (4) fixation of part of the nitrogen around the veins (as revealed by the observed enriched values). Nitrogen enrichment has been found to correlate significatively with base metal sulphide mineralization in countries such as Peru and Mexico among others (Appleton et al. 1989). Another point to be considered is the isotopic signature of some of the deposit's sulphides. $\delta^{34}S$ preliminary studies in stibnite (stage H2) and pyrite (stage H3) reveal mean values of $0.3‰$ ($n = 4$) and $-3.9‰$ ($n = 2$) (Ortega 1993), that closely match the typical values for igneous sulphur. In this sense it can be argued that the intrusion of the Alburquerque batholith played a key role in the hydrothermal processes. Sulphur was most probably supplied by the igneous body either by magmatic fluids or leached by heated solutions of meteoric origin.

With regards to the origin of metals, antimony enrichment in the alteration zones implies that hydrothermal fluids introduced metals to the host rocks from an external source. The high positive correlations between Sb and Mo in Mari Rosa ($r \approx 1$ in the stibnite veins, $r = 0.9$ in the host rocks) might indicate a genetic link between both elements. Since Mo is an element typically associated with acid igneous intrusions (Uzkut 1974; Oyarzún 1978; Oyarzún 1984) the same source could be inferred for Sb i.e., the Alburquerque batholith. On the contrary Mo and Au have reverse distribution trends, with gold becoming depleted in highly differentiated magmas (Gottfried et al. 1972; Tilling et al. 1973; Oyarzún 1984). However, this type of magmatism creates the conditions adequate enough to mobilize gold out of the rocks hosting the intrusion (Oyarzún 1984). Thus, we might expect in this case that gold was actually leached from the Schist Greywacke Complex rocks, put into solution as a complex ion and later introduced and precipitated within the veins.

Depth of mineral deposition

The pressure estimate for the boiling event at Mari Rosa is 0,9–1 kbar (Ortega et al. 1991a,b; Ortega 1993). If pure hydrostatic conditions are considered, ore deposition could have occurred as deep as 9–10 km (Yerkes et al. 1985; Gregory and Backus 1980; Wood and Walther 1986; Sibson 1990). However the geological and structural framework suggest that this assumption might be incorrect:

1. An area subjected to widespread plutonic activity would have an anamalously high geothermal gradient ($\gg 30°$/Km). Thus, a depth of 9–10 km would have resulted in much higher temperatures than the ones observed in Mari Rosa (≈ 300 °C).
2. Contrary to the case of deep high-angle faults (e.g. Sibson 1987; Sibson et al. 1988), the structural style of Mari Rosa V_o veins i.e., small low-angle thrusts, would have prevented any connection between the depositional site and the surface. This idea is also supported by the preservation of vapor within the system (trapped as type III inclusions) during boiling, thus indicating a system closed to the surface.
3. Furthermore, depth values of 10 km are too high to maintain pure hydrostatic pressure (Sibson 1990; Jebrak 1992). In this sense, pure hydrostatic conditions can be ruled out. The alternative (lithostatic or quasi lithostatic conditions) would indicate more realistic values of 4 km (pure lithostatic conditions) to 5 km (quasilithostatic conditions) (Yerkes et al. 1985; Gregory and Backus 1980; Wood and Walther 1986; Sibson 1990).

Transport and precipitation of antimony

The dominance of hydroxothioantimonite over thioantimonite is clear within the range 275°–350 °C (Krupp 1988), a temperature range compatible with the values estimated for Mari Rosa. However, precipitation of stibnite from hydroxoanthimonite seems incompatible with a precipitation mechanism such as boiling. It is generally accepted that boiling would lead to degassification (Drummond and Ohmoto 1985), resulting in H_2S being lost to the system. This process would increase the solubility of hydroxoanthimonite thus preventing the precipitation of stibnite:

$$\tfrac{1}{2}\,Sb_2O_3 + H_2O = \tfrac{1}{2}\,Sb_2S_2(OH)_2 + H_2S \text{ (Krupp 1988)}$$

However, three factors must be taken into account:
1. There is clear evidence of boiling in the system; furthermore, close textural relationships between quartz formed during this process and stibnite indicate that they are coeval.
2. The structural frame of Mari Rosa (e.g. V_o veins) indicates that mineral precipitation was rather confined to dilational cavities (jogs) developed along low-angle thrusts, which would have prevented a generalized vapor loss during boiling. This is the opposite to what is observed in shallow, open systems such as geothermal fields, where mineralization tend to concentrate along or near to high-angle normal faults acting as preferred conduits for fluid circulation and open air discharge of solutions and volatiles (e.g. Henley 1985; Henley and Brown 1985).
3. In a complex system such as the one under study, the tendency of the different components is to concentrate within the volatile fraction is the following $H_2S < CO_2 < CH_4 < N_2$ (Ramboz et al. 1982).

Thus, if no significant H_2S escaped from the hydrothermal fluid, the main argument against boiling and precipitation of Sb out of hydroxoanthimonite (i.e., H_2S degassification) can be ruled out. Then, it can be argued that:

(1) antimony was transported as $Sb_2S_2(OH)_2$ (or polymers of composition $Sb_{2n}S_{3n-1}(OH)_2$; Krupp 1988), and (2) Sb_2S_3 precipitated as massive ore during boiling within highly confined structures. This idea, as discussed above, is largely consistent with the structural and textural evidence, fluid inclusion data, thermodynamic considerations and experimental data on Sb complexing at higher temperatures.

Finally, regarding redox conditions during mineral precipitation, Ramboz et al. (1985) and Dubessy et al. (1987) have proposed the possibility of estimating the fO_2 from the molar volume and composition of the fluid. This calculation is based on the assumption that chemical equilibrium $CO_2 + 2H_2O \rightleftharpoons CH_4 + 2O_2$ occurs in the hydrothermal system. Since in Mari Rosa the fluid evolves towards a total loss of CO_2 (stage H3; Table 5) a decrease in the oxidation state could be inferred. However, both mineralogical and isotopic evidence suggest the opposite: (1) precipitation of carbonates takes place only during the final stage, and (2) the sulphur isotopic composition shifts towards lighter values (Ortega et al. 1994), which according to Ohmoto (1972) implies more oxidizing conditions. Furthermore, as stated by Ohmoto and Lasaga (1982) and Drummond and Ohmoto (1985), equilibria involving sulphide and sulphate ($H_2S + 2O_2 \rightleftharpoons HSO_4^- + H^+$) are considerably more important in establishing the redox state of typical boiling hydrothermal fluids than the extremely sluggish reaction between CO_2 and CH_4.

Conclusions

The Mari Rosa deposit is the result of a metallogenic process involving complex fluid-rock interactions. Geological and geochemical evidence indicate that the batholith of Alburquerque played a major role in these processes. This late Hercynian intrusion triggered hydrothermal activity and possibly contributed metals (Sb) and sulphur to the system. Contact metamorphism around the intrusion might have created optimum conditions to liberate nitrogen from the country rocks. The elements were transported and deposited in three hydrothermal stages, the second of which is the most important and resulted in massive stibnite-gold deposition. Hydrothermal alteration around the veins was mild and consisted in chloritization, carbonatization and sericitization. Fluids associated with ore deposition were mainly aqueous, moderately saline with CH_4-N_2-CO_2 as volatile components. They evolved, progressively cooling from initial circulation temperatures close to 400 °C to around 150 °C in the late episode. In conjunction with this, the fluid composition evolution was characterized by a progressive increase in the global water content of the fluids, along with an increase in the relative proportion of N_2 with respect to CH_4 and CO_2 in the volatile fraction. Only the second hydrothermal stage was an important mineralizing episode, with massive stibnite deposition resulting from a boiling process developed at 300 °C and 0.9–1 kbar. Unmixing of the fluid was induced by a sudden pressure drop in the V_o dilational jogs during low-angle fault movement. Pressure conditions together with geological evidence suggest mineral deposition under lithostatic or quasi-lithostatic conditions implying a depth of 4–5 km.

Acknowledgements. This research was funded by the Spanish Ministry of Education through a post-graduate scholarship. We acknowledge assistence from Southampton University (Geology Department), namely Drs. I.W. Croudace, S. Roberts, J. Marshall and Ms. P. Boella, for providing facilities and advice on analytical techniques. Sulphur isotope analyses were performed by Dr. E. Cardellach at Yale University. The structural interpretation benefited from the comments of Dr. M. Doblas (C.S.I.C., Madrid). The authors appreciate the helpful discussions on fluid inclusion studies with Drs. J. Touret and A.M. van den Kerkhof (Free University, Amsterdam). Grammar and syntax benefited from a comprehensive revision of the manuscript by Dr. J. McGowan.

References

Abalos, B., Eguiluz L. (1992) Geología estructural del Corredor Blastomilonítico de Badajoz-Córdoba. Bol. Geol. Min., 103(1): 3–41

Appleton, J.D., Ridgway, J., Claros J., Gomez Caballero, A., Rodríguez, W., Villaseñor, M.G. (1989) Lithogeochemical exploration for silver mineralization in Bolivia, Mexico and Peru. Trans. Inst. Min. Metall. 98: 201–212

Armbrust, G., Oyarzún, J., Arias, J. (1977) Rubidium as a guide in Chilean porphyry copper deposits. Econ. Geol. 72: 1086–1100

Arribas, A., Arribas Rosado, A., Gumiel, P., Martin-Izard, A., Reguilón R. (1987) Caracteres metalogénicos de los yacimientos asociados a los granitoides del Macizo Hespérico. In: F. Bea, A. Carnicero, J.C. Gonzalo, M. López Plaza, M.D. Rodriguez (ed.) Geología de los granitoides y rocas asociadas del Macizo Hespérico. Ed. Rueda, Madrid, Spain, pp. 233–263

Bascones, L., Martín Herrero, D. (1982) Mapa Geológico de España, E/1: 50000. Hoja 674–675, Sever-Santiago de Alcántara. Instituto Geológico y Minero de España, Madrid, Spain

Boiron, M.C., Cathelineau, M., Dubessy, J., Bastoul, A.M. (1990) Fluid in the Hercynian Au-veins from the French Variscan belt. Min. Mag. 54: 231–243

Boyle, R.W. (1974) The use of major elemental ratios in detailed geochemical prospecting utilizing primary haloes. J. Geochem. explor. 3: 345–369

Boyle, R.W. (1979) The geochemistry of gold and its deposits. Can. Geol. Sur. Bull. 280: 584 pp

Boyle, R.W. (1982) Chemical methods for the discovery of blind mineral deposits. C.I.M. Bull. 75–844: 113–142

Cruzat, A. (1984) Prospección geoquímica aplicada a yacimientos de Au. Rev. Geol. de Chile 21: 53–75

Drummond, S.E., Ohmoto, H. (1985) Chemical evolution and mineral deposition in boiling hydrothermal systems. Econ. Geol. 80: 126–147

Dubessy, J., Ramboz, C. (1986) The history of organic nitrogen from early diagenesis to amphibolite facies: mineralogical, chemical, mechanical and isotopic implications. In: Proc. 5th Int. Symp. Water-Rock Interaction, Reykjavik, Iceland, pp. 170–174

Dubessy, J., Ramboz, C., Nguyen-Trung, C., Cathelineau, M., Charoy, B., Cuney, M., Leroy, J., Poty, B., Weisbrod, A. (1987) Physical and chemical controls (fO_2, T, pH) of the opposite behaviour of U and Sn-W as examplified by hydrothermal deposits in France and Great Britain, and solubility data. Bull. Minéral. 110: 261–281

Gallego, M. (1992) Las mineralizaciones de litio asociadas a magmatismo ácido en Extremadura y su encuadre en la Zona Centro Ibérica. Ph.D. Thesis Universidad Complutense, Madrid, Spain, 323 pp

Gallego, M., Gumiel, P. (1993) Li-minerlization at Tres Arroyos (Alburquerque, Badajoz) as a result of the mineralogical and geochemical evolution of the Alburquerque batholith. Geogaceta 13:29–32

González-Bonorino, F. (1971) Metamorphism of the crystalline basement of Central Chile. J. Petrol. 12:149–175

Gottfried, D., Rowe, J.J., Tilling, R.E. (1972) Distribution of gold in igneous rocks. US Geological Survey Prof. Pap., 727, 42 pp

Gregory, A.R., Backus, M.M. (1980) Geopressured formation parameters, geothermal well, Brazoria County, Texas. In: Dorfman, M.H., Fisher, W.L. (eds.) Proc. 4th U.S. Gulf Coast Geopressure-Geothermal Energy Conf. 1:235–311

Guillot, C. (1989) Origine et comportement de l'azote dans les formations metamorphiques: Etude des inclusions fluides et géochimie de l'ammonium dans le dôme de Montredon (Montagne Noire, France). Ph.D. Thesis Université Paul Sabatier, Toulouse, France, 239 pp

Gumiel, P. (1983) Metalogenia de los yacimientos de Sb de la Península Ibérica. Tecniterrae 27:6–120

Gumiel, P., Arribas A. (1987) Antimony deposits in the Iberian Peninsula. Econ. Geol. 82:1453–1463

Gumiel, P., Gallego, M. (1991) Other prospects. In: Gumiel, P., Antón-Pacheco, C., Campos, R. (eds.) Development of new multi-disciplinary techniques for mineral exploration in several areas of the Western Iberian Peninsula. Spec. Pub. Bol. Geol. Min. Instituto Geológico y Minero, Madrid, Spain, pp. 43–53

Gumiel, P., Arribas, A., Saavedra, J. (1976) Geologia y metalogenia del yacimiento de estibina-scheelita de San Antonio, Alburquerque, Badajoz. Stvdia Geol. 10:61–93

Hall, A., Bencini, A., Poli, G. (1991) Magmatic and hydrothermal ammonium in granites of the Tuscan magmatic province, Italy. Geochim. Cosmochim. Acta 55:3657–3664

Hallam, M., Eugster, H.P. (1976) Ammonium silicate stability relations. Cont. Min. Petrol. 57:227–244

Henley, R.W. (1985) The geothermal framework of epithermal deposits. In: Berger, B.R., Bethke, P.M. (eds.) Geology and geochemistry of epithermal systems. Reviews in Economic Geology, vol. 2. Society of Economic Geologists, University of Texas at El Paso, USA, pp. 1–24

Henley, R.W., Brown, K.L. (1985) A practical guide to the thermodynamics of geothermal fluids and hydrothermal ore deposits. In: Berger, B.R., Bethke, P.M. (eds.) Geology and geochemistry of epithermal systems. Reviews in Economic Geology, vol. 2. Society of Economic Geologists, University of Texas at El Paso, USA, pp. 25–44

Jebrak, M. (1992) Les textures intra-filoniennes, marqueurs des conditions hydrauliques et tectoniques. Chron. Mines. Rech. Miniere 506:25–35

Kerkhof, A.M. van den (1988) The system CO_2-CH_4-N_2 in fluid inclusions: theoretical modelling and geological applications. Ph.D. Thesis, Free University of Amsterdam, Amsterdam, The Netherlands, 206 pp

Kreulen, R., Schuiling, R.D. (1982) N_2-CH_4-CO_2 fluids during formation of the Dôme de l'Agout, France. Geochim. Cosmochim. Acta 46:193–203

Krupp., R.E. (1988) Solubility of stibnite hydrogen sulfide solutions, speciation, and equilibrium constants from 25 to 325 °C. Geochim. Cosmochim. Acta 52:3005–3015

La Roche, H., Marchal, M. (1978) Leucogranites et granites du Massif de Valencia de Alcantara (Espagne). Sci. Terre 22:181–200

López Plaza, M., Martinez Catalán, J.R. (1987) Sintesis estructural de los granitoides hercinicos del Macizo Hespérico. In: F. Bea, A. Carnicero, J.C. Gonzalez, M. Lopez Plaza, M.D. Rodriguez (ed.) Geologia de los granitoides y rocas asociadas del Macizo Hespérico. Ed. Rueda, Madrid, Spain, pp. 195–210

Miyashiro, A. (1978) Metamorphism and metamorphic belts. Allen & Unwin, Boston, 491 pp

Ohmoto, H. (1972) Systematics of sulfur and carbon isotopes in hydrothermal ore deposits. Econ. Geol. 67:551–578

Ohmoto, H., Lasaga, A. (1982) Kinetics of reactions between aqueous sulfates and sulfides in hydrothermal systems. Geochim. Cosmochim. Acta 46:1727–1745

Ortega, L. (1993) Caracterización de los procesos hidrotermales en las mineralizaciones de antimonio de Mari Rosa y El Juncalón (Zona Centro Ibérica meridional). Ph.D. Thesis Universidad Complutense, Madrid, Spain, 386 pp

Ortega, L., Vindel, E., Dubessy, J. (1991a) Fluid evolution in a boiling system around a cooling granite: a Hercynian antimony deposit case study. Plinius 5:162–163

Ortega, L., Vindel, E., Beny, C. (1991b) C-O-H-N fluid inclusions associated with gold-stibnite mineralization in low-grade metamorphic rocks, Mari Rosa mine, Caceres, Spain. Mineral. Mag. 55:235–247

Ortega, L., Oyarzun, R., Gallego, M., Lillo, J. (1994) Geoquimica de los procesos de alteración hidrotermal en la mineralización de Sb de Mari Rosa (Zona Centro Ibérica). Estud. Geol. 50:143–168

Oyarzún, J. (1974) Rubidium and strontium as guides to copper mineralization emplaced in some Chilean andesitic rocks. J. Geochem. Explor. 3:333–338

Oyarzún J. (1978). Geochemistry of Molybdenum. In: Sutulov, A. (ed.) International Molybdenum Encyclopaedia, 1778–1978, vol. I. Resources and production: Intermet publications, Santiago de Chile, pp. 154–173

Oyarzún J. (1984) Geoquimica y metalogénesis endógena del oro. Rev. Geol. Chile 21:3–10

Oyarzún, R. (1982) Geology and geochemistry of the Banded Iron Formations in the Nahuelbuta Mountains, Chile. PhD Thesis University of Leeds, Leeds, UK, 226 pp

Penha, M.H., Arribas, A. (1974) Datación geocronológica de algunos granitos uraniferos españoles. Bol. Geol. Min. 85: 271–273

Pérez Cerdán, F., Garcia de Santiago, P., Antón-Pacheco, C., Gumiel, J.C. (1991) Integration of data using a geographical information system. In: Gumiel, P., Antón-Pacheco, C., Campos, R. (eds.) Development of new multi-disciplinary techniques for mineral exploration in several areas of the Western Iberian Peninsula. Spec. Pub. Bol. Geol. Min. Instituto Geológico y Minero, Madrid, Spain, pp. 81–86

Potts, P.J., Tindle, A.G., Webb P.C. (1992) Geochemical Reference Material Compositions. Whittles, London UK, 313 pp

Quesada, C., Florido, P., Gumiel, P., Osborne J. (1987) Memoria del Mapa Geológico y Minero de Extremadura, E/1:300 000, Junta de Extremadura; Consejeria de Industria y Energia; Dirección General de Industria, Energia y Minas, Merida, Spain

Ramboz, C., Schnapper, D., Dubessy, J. (1985) The P-V-T-X-fO_2 evolution of H_2O-CO_2-CH_4-bearing fluid in a wolframite vein: reconstruction from fluid inclusion studies. Geochim. Cosmochim. Acta 49:205–219

Roberts, S., Sanderson, D., Dee, S., Gumiel, P. (1991) Tectonic setting and fluid evolution of auriferous quartz veins from the La Codosera area, SW Spain. Econ. Geol. 86:1012–1022

Santos, J.A., Casas J. (1982) Memoria Explicativa del Mapa Geológico de España, E/1: 50 000, Hoja 727, Alburquerque. Intituto Geológico y Minero de España, Madrid, Spain, 33 pp

Serrano Pinto, M., Casquet, C., Ibarrola, E., Corretgé, L.G., Portugal Ferreira, M. (1987) Sintese geocronologica dos granitoides do Maciço Hesperico. In: F. Bea, A. Carnicero, J.C. Gonzalez, M. Lopez Plaza, M.D. Rodriguez (ed.) Geologia de los granitoides y rocas asociadas del Macizo Hespérico. Ed. Rueda, Madrid, Spain, pp. 69–86

Shaw, D. (1956) Trace elements in pelitic rocks. Part III. Major elements and general geochemistry. Geol. Soc. Am. Bull. 67:919–934

Sibson, R.H. (1987) Earthquake rupturing as a mineralizing agent in hydrothermal systems. Geology 15:701–704

Sibson, R.H. (1990) Faulting and fluid flow. In: Nesbitt, B.E. (ed.) Short Course on Fluids in Tectonically Active Regimes of the Continental Crust. Mineralogical Association of Canada, Vancouver, Canada, pp. 93–129

Sibson, R.H., Robert, F., Howard Poulsen, K. (1988) High-angle reverse faults, fluid-pressure cycling, and mesothermal gold-quartz deposits. Geology 16:551–555

Spycher, N.F., Reed, M.H. (1989) Evolution of a Broadlands-type epithermal ore fluid along alternative P-T paths: implications for the transport and deposition of base, precious and volatile metals. Econ. Geol. 84:328–359

Steed, G.M., Morris, J.H. (1986) Gold mineralization in Ordovician Greywackes at Clontibret, Ireland. In: Duncan, K.J., Boyle, R.W., Haynes, S.J. (eds.) Turbidite hosted gold deposits. Geol. Assoc. Can. Spec. Pap. 32:67–86

Swanenberg, H.E.C. (1980) Fluid inclusions in high-grade metamorphic rocks from SW Norway. Geologica Ultraiectina, vol. 25. University of Utrecht Press, Utrecht, 146 pp

Tatlock, D., Flanagan, F., Bastron, H., Berman, S., Sutton A. (1976) Rhyolite RGM-1 from Glass Mountain, California. U.S.G.S. Prof. Pap. 840:11–14

Taylor, S.R., McLennan, S.M. (1985) The continental crust: its composition and evolution. Blackwell, Oxford, 312 pp

Tilling, R.I., Gottfried, E., Rowe, J.J. (1973) Gold abundance in igneous rocks: bearing on gold mineralization. Econ. Geol. 68:168–186

Turekian K. y Wedepohl K. (1961). Distribution of elements in some major units of the Earth's crust. Bull. Geol. Soc. Am. 72:175

Uzkut, I. (1974) Zur Geochemie des Molybdäns. Bontraeger, Berlin, 226 pp

Wilkinson J.J. (1991) Volatile production during contact metamorphism: the role of organic matter in pelites. J. Geol. Soc. London. 148:731–736

Wood, B.J., Walther, J.V. (1986) Fluid flow during metamorphism and its implications for fluid-rock ratios. In: Walther, J.V., Wood, B.J. (eds.) Fluid rock interactions during metamorphism. Advances in Physical Geochemistry, vol. 5. Springer Berlin Heidelberg New York, pp. 89–108

Yerkes, R.F., Levine, P., Wentworth, C.M. (1985) Abnormally high fluid pressures in the region of the Coalinga earthquakes – a preliminary report. U.S. Geol. Surv. Open-File Rep. 85–44: 344–375

Editorial handling: I. Ryabchikov